

Implementation of “MSG-3” for Crack Growth Analysis of Aircraft SSI Components

A. R. Nikouee^{1*} and S. Adibnazari²

1, 2. Department of Mechanical and Aerospace Engineering, Science and Research Branch, Islamic Azad University

Postal Code: 1477893855, Tehran, IRAN

*arncao@yahoo.com

The main goal of this article is to implement the MSG-3 process in structure field for an SSI component of b747 aircraft. This process is expected to increase the ease of aircraft maintenance and its safety level. MSG-3 logic took a top-down or consequence of failure approach meaning that MSG-3 reduces the maintenance cost and upgrades safety. Moreover, it can significantly help saving the time and providing financial benefits for the design approach and the development of maintenance programming. In this study, in correspondence with the SLD of MSG-3, an SSI component is selected and its fatigue crack growth analysis is investigated. The approach of this study is to use the FEM and fractography for the purpose of exploring the loading.

Keyword: SSI Components, Aircraft, Crack, Analysis

Nomenclature

AD	Accidental Damage
ATA	Air Transport Association
ED	Environmental Deterioration
EFT	Extended Fatigue Testing
FAA	Federal Aviation Administration
FCG	Fatigue Crack Growth
FD	Fatigue Damage
FDA	Fatigue Damage Analysis
FEM	Finite Element Method
FS	Fatigue Striation
GLS	Generic Load Spectrum
LC	Load Crack
LDD	Logic Decision Diagram
LDP	Logical Decision Processes
MRB	Maintenance Review Board
MSG-3	Maintenance Steering Group 3
NDI	Non Destructive Inspection
NDT	Non Destructive Testing
OEM	Operation Empty Weight
OEW	Operation Empty Weight
SI	Structural Integrity
SIF	Stress Intensity Factor
SLD	Structural Logic Diagram
SSI	Significant Structural Item

TDI

Tear Down Inspection

Introduction

The definition of maintenance in industry generally includes those tasks required to restore or maintain an aircraft systems, components, and structures in an airworthy condition [1]. Airline and manufacturer experience in developing scheduled maintenance for new aircraft has shown that more efficient programs can be developed through the use of LDP [2]. The work of ATA task force led to the development of a new, task-oriented maintenance process defined as MSG-3 [1]. One of the main parts of the MSG-3 process is structural treatment. In this treatment, the structural logic evolves into a form which more directly assesses the possibility of structural deterioration processes. Considerations of fatigue, corrosion, accidental damage, age exploration, and others are incorporated into the logic diagram and are routinely considered [2]. This section contains guidelines for developing scheduled maintenance tasks for aircraft structure designed to relate scheduled maintenance tasks to the consequences of structural damage that remain undetected. Each structural item is assessed in terms of its significance to continuing airworthiness, susceptibility to any form of damage, and the degree of difficulty involved in detecting such damage. Once this is established, scheduled structural maintenance can be developed which can be effective in detecting

1. PhD Candidate (Corresponding Author)

2. Professor

and preventing structural degradation due to fatigue, environmental deterioration, or accidental damage throughout the operational life of the aircraft. The structural maintenance task(s) are developed as part of the scheduled structural maintenance [2]. In this study, the aircraft SSI component of a Boeing 747 was selected for assessment of crack growth using SLD, implementing crack growth analysis through the experimental study of fatigue crack. Smaller cracks were investigated with fractography and lead cracks were investigated using "FEM". Upon part selection, the general spectrum of loading was defined, and after designating loading spectrum, with the aid of modeling, fatigue crack growth and the element design were analyzed based on the finite element method.

Background

MSG-3 Development

In 1968 the MSG was created with a mandate to formulate an LDP for development of the initial scheduled maintenance requirements for new aircrafts. That same year, representatives of the steering group developed "MSG-1" which, for the first time, used an LDD to develop the scheduled maintenance program for the new Boeing 747 aircraft. In 1970, MSG-1 was updated to MSG-2 to make it applicable for later generations of aircraft. MSG-2 decision logic was subsequently used to develop scheduled maintenance programs for the aircraft of the 1970s.

In 1979, the ATA task force sought to improve on MSG-2 in order to address a new generation of advanced technology aircraft (B757 and B767)[1]. The work of the ATA task force led to the development of a new task-oriented maintenance process defined as MSG-3[1]. Today, MSG-3 is the only method used by commercial airplane manufacturers. Policy states that the latest MSG analysis procedures must be used for the development of routine scheduled maintenance tasks for all new or derivative aircraft. In MSG-3, the structural inspection program is designed to provide timely detection and repair of structural damage occurring during commercial operations. Detection of damages such as corrosion and fatigue cracking by visual and/or NDT procedures are considered [1]. The primary objective of the scheduled structural maintenance is to maintain the inherent airworthiness throughout the operational life of the aircraft in an economical manner. To achieve this, the inspections must meet the detection requirements of each of the AD, ED and FD assessments. Inspections related to the detection of AD/ED are applicable to all aircraft when they first enter service [2]. Also inspections related to FD detection in metals are applicable after a threshold [2]. Additionally, accidental Damage (AD) is characterized by the occurrence of a random discrete event [2]. Besides, Environmental Deterioration (ED) is

characterized as structural deterioration resulting from a chemical interaction with its climate or environment [2]. Finally, Fatigue Damage (FD) is described as the initiation of a crack or cracks due to cyclic loading and subsequent propagation [2]. Moreover, in order to increase the level of safety and economical gain for operators as well as manufactures and to ease the oversight of authorities in the structural division, at first all aircraft structural elements should be classified. Secondly, the group classification of the types of inspections and maintenance intervals has to be examined. The above-mentioned elements consist of [2]:

1. SSI which in fact are primary structural parts of the aircraft. A Structural Significant Item (SSI) is any detail, element or assembly, which contributes significantly to carrying flight, ground, pressure or control loads, and the failure of which could affect the structural integrity necessary for the safety of the aircraft [2].
2. Other elements, known as "Other Structure", is judged not to be a structural Significant Item. It is defined both externally and internally within zonal boundaries [2].

The structural logical diagram "SLD" in the MSG-3 process is shown in Fig. 1.

Extended Fatigue Testing

Between 2002 to 2005 three articles were published by Bakuckas and Carter (2002 -2003) and Mosinyi, Bakuckas, Ramakrishnan, and Lau-Tan-Awerbuch (2005) on extended fatigue testing on some parts of a scrapped Boeing 727 (i.e. extended fatigue testing to evaluate the structural integrity of high age aircraft) [3,4,5]. In fact these articles were the result of a common project accomplished by a team of representatives from the Federal Aviation Administration, Delta Airlines, and Drexel University which lasted four years and involved tear-down inspection and extended fatigue testing on a scrapped Boeing 727 structure with the total cycle equal to 60000 [3,4,5]. These activities were accomplished on suspected widespread crack growth points, and for this purpose, eleven aircraft fuselage panels were dismantled from the aircraft; seven panels with unique damage were investigated by Non-destructive testing (NDT) and the four remaining uniquely damaged panels were examined in an FAA-approved laboratory under complete aircraft fuselage testing [3,4,5]. In fact, possible existing cracks and crack growth during this test were actively inspected. There were no signs of crack after 43500 simulated flight cycles (FC). In an aircraft which was equal to 60,000 cycles before being completely scrapped, after 104,000 flight cycles on the test panel, there was no sign of crack [3, 4, 5].

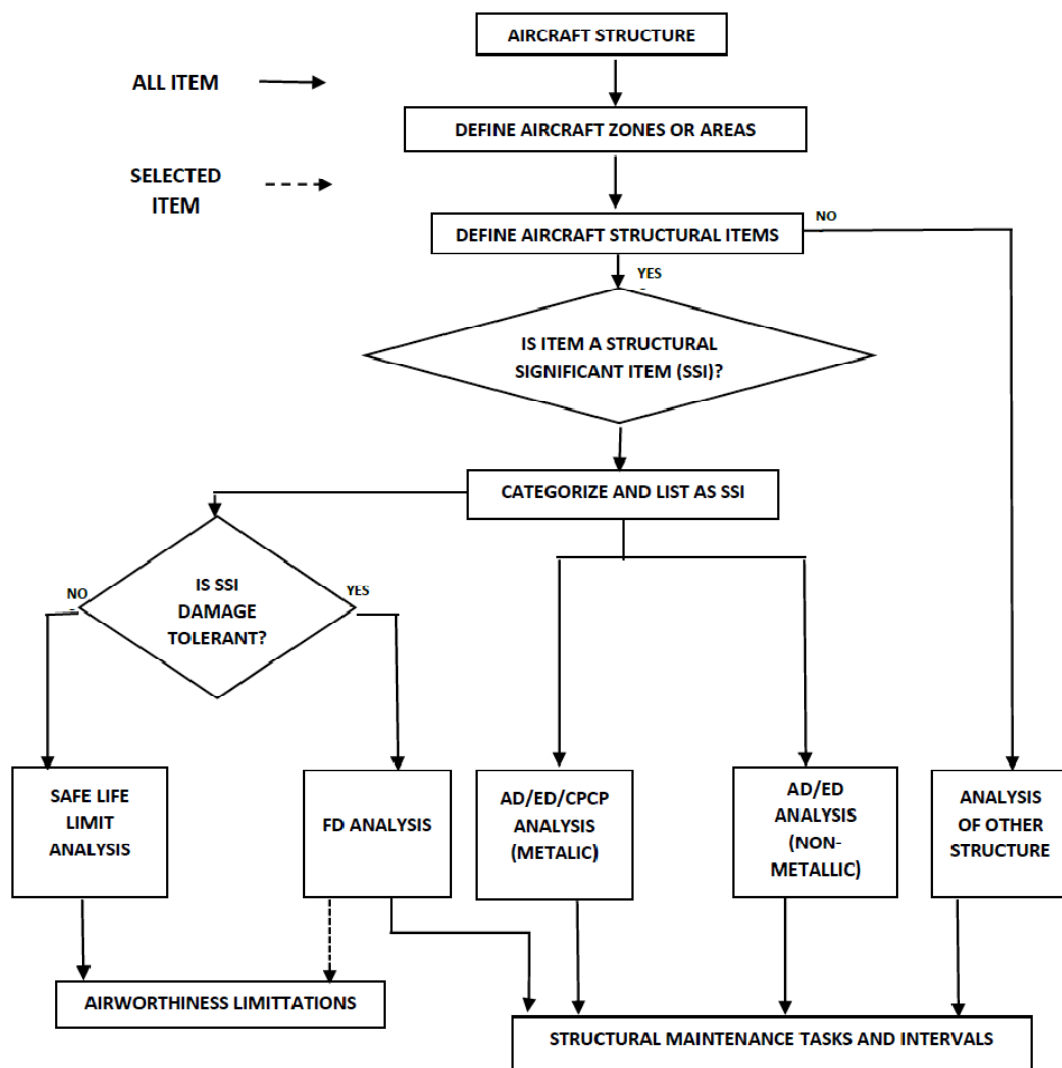


Figure 1. SLD in MSG-3 process

Theoretical Investigation

Introduction of the Part to be investigated

As mentioned in the previous section, the main goal of this study was to implement the MSG-3 process on selected SSI elements of a Boeing 747 aircraft. The study focused on a part of the structure and according to the SLD and MSG-3 process, the intended part was designated through a structure logic diagram. The selected SSI parts of a Boeing 747; with accumulated 16756 FC and 64555 FH were removed from section 41 of this aircraft and located on Frame Station 300[6]. The main task in this study was to investigate crack growth rate in crack locations, in a defined direction and under a specified default loading spectrum. Figs. 2 through 4 are illustrations of the part under investigation. A hole is shown in one of these areas. The general form of these cracks for the selected part is shown in detail in Fig. 4.

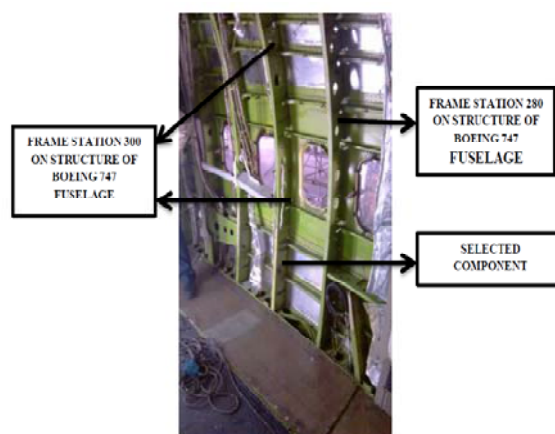


Figure 2. The image of frame station 300, 280 and selected component on aircraft fuselage



Figure 3. Image of selected component at frame STA. 300



Figure 4. The exact location of the crack under test analysis

Surface Cracks Fractography

Fractography is a method of analyzing damage and failure (fatigue, corrosion, and other similar phenomena). Because of surface fraction, this method is used to investigate and show damage and failure signs, as reported in the 1951 articles issued by Zaffe and Worden specifically focusing on “fatigue striation” [7].

Although “Orowan” announced that a great number of cyclic operations are required to start initial fatigue crack at a critical position, Forsyth and Ryder could show fatigue crack in each loading cycle by using an optical microscope and one aluminum fatigue crack sample. They established a one-to-one correspondence between the number of fracture striation found in each loading cycle and number of cyclic load. They also presented reasonable evidence for crack growth rate and fatigue crack propagation in each loading cycle as a result of fracture striation configuration. Not only this result has a significant role in determining fatigue crack growth property, but it also provides a situation in which loading history on a part can be defined by counting fracture striation in the defined space and distance [7]. In relation to form of fracture striation, fatigue crack growth mechanism was designated by Laird, Smith, McMillan, Pelloux, Schijve, Nix and Flower, and also McEvily and Matsunaga; who declared that there was no evidence to confirm fatigue crack growth in either steel or aluminum alloy unless in a cycle-by-cycle base. Consequently, if there was no sign of fracture striation,

there would be some other causes, such as accident, for damage and failure analysis. Hence, it was necessary to designate their mechanism and situation of occurrence and define the part operation condition and surface fracture specification, especially for brittle and smooth materials [7].

Mechanism for the introduction of aircraft structural elements failure which could be investigated are short-term loading, fatigue, corrosion, or creeping; however, it is possible to see surface fractures, the inspection of which is done by fractography. The main tools in fractography are the x-ray, electronic microscope, and similar equipment [7]. In this study, the electronic microscope used was LEO 440i. In order to investigate surface fractures on selected part cracks; an electronic microscope (SEM) (Fig 5) was used for fractography. Figs. 6, 7, and 8 are related to a small crack on the part (Fig 4 the smallest crack is located on the left side of the hole). Crack growth rate for this mode is given in Table 1. The first column is the crack size from the first edge of fracture surface, the second column is the exact location of striation from the first edge of fracture surface, the third column is the number of striation being considered, and fourth column is crack growth rate. Figs. 9, 10, and 11 show the large crack surface fractography. Fractography of this surface fracture showed that the lead crack initiation resulted from fatigue striation; but there was no surface fracture on the fractography. Therefore surface friction from rubbing was one of the reasons. Although fatigue panels and crack growths were possible reasons for crack initiation, accidental damage triggered this situation. Therefore, fatigue crack analysis was accomplished by assuming crack growth resulting from fatigue.

Table 1. The result of fractography around smaller cracks

$a(mm)$	Distance on fracture surface (μm)	Number of fatigue striation	$\frac{da}{dN}(\frac{\mu m}{cycle})$
8	26.6	18	1.49
8.8	15	8	1.87
9.3	10.7	5	2.14



Fig 5. Electronic microscope used for the project fractography

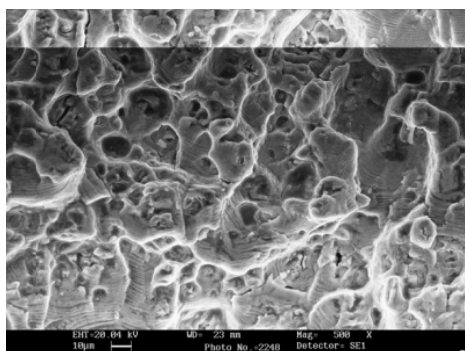


Figure 6. Fatigue striation at 8 mm of crack initiation point with 500 times magnification

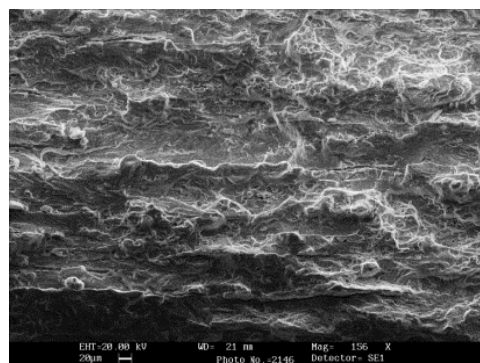


Figure 10. Fatigue striation at 6.3mm of crack initiation point with 1560 times magnification

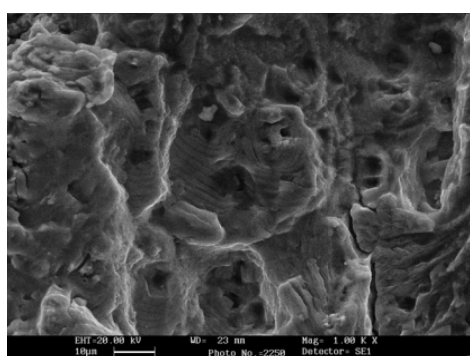


Figure 7. Fatigue striation at 88mm of crack initiation point with 1000 times magnification

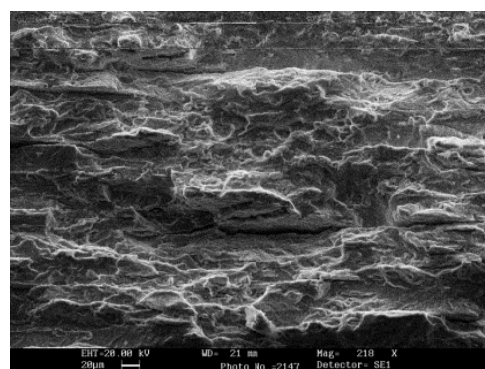


Figure 11. Fatigue striations at 25.3mm of crack initiation with 2180 times magnification

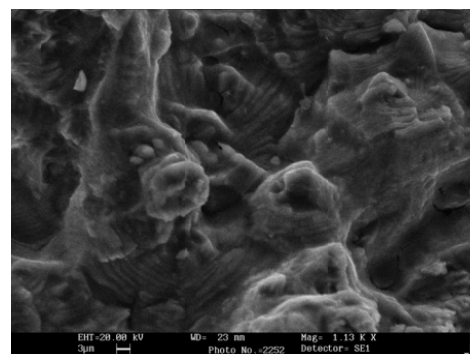


Figure 8. Fatigue striation at 9.3 mm of crack initiation point with 1130 times magnification

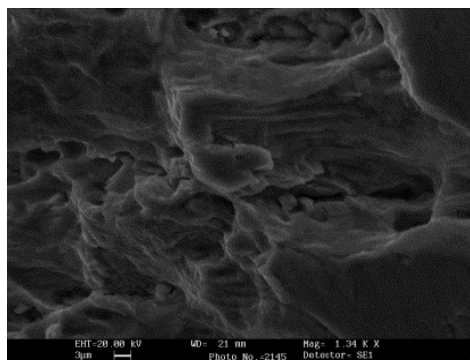


Figure 9. Fatigue striation at 2mm of crack initiation point with 1134 times magnification

Loading

In order to perform fatigue crack growth analysis, as illustrated in Figs. 5 and 6, the bigger cracks are analyzed using the finite element method. For this purpose, the first stage was to designate loading indicators. As it is a complicated task to designate specification of applied loading during different stages of flight, a reference was used to define the loading sample for large commercial aircraft and to designate the general load spectrum, which was then utilized as a general model of loading history. Parameters used to define loading included: intended aircraft dimensions, empty operation weight, maximum payload capacity, and aircraft operation data such as ranges of flight, cruising level, cruising speed, takeoff speed, landing speed, fuel consumption as well as the trend of differential cabin pressure variations, aircraft flight history and aircraft reaction in wind gusts [8]. Each loading spectrum consisted of the continued loading of 6000 flight cycles, which was a combination of the variable coefficient of loading (Δg) in the aircraft's center of gravity and differential cabin pressure, which was related to flight altitude. The number of flights in a spectrum was one-tenth of the maximum designed service life of a wide-bodied jet aircraft, as the service life of such aircraft is typically defined as 60,000 flights. The regular flight profile of commercial

aircraft is divided into different stages, which are shown in Fig. 12 and named in table 2 [8].

Table 2. Load Environment at Each Stage of Flight Profile

Stage no.	Stage	Load environment
1	Preflight Taxi	Taxi Ground
2	Takeoff Run	Ground
3-8	Climb	Gust and Maneuver
9	Cruise	Gust and Maneuver
10-15	Descent	Gust and Maneuver
16	Landing	Landing Impact
17	Landing Roll	Roll Ground
18	Postflight Taxi	Taxi Ground

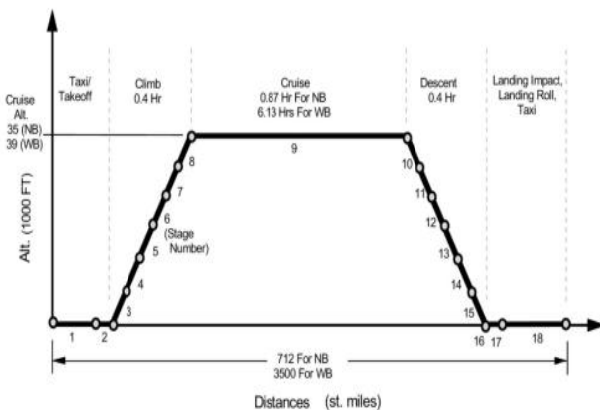


Figure 12. Ordinal diagram for stages of flight profile

In different flight modes shown in Fig. 12 and named in table 2, the circumferential loading which could affect fuselage structure was divided into four groups [8]:

- Aircraft flight maneuvering in different cruise, climb, and landing stages
- Aircraft ground operations including aircraft preflight movement, consistent surface movement, taxiing, the landing phase, and landing impact
- Wind gust loading during weather deterioration.
- Internal cabin pressure

The first three circumferential loadings (which were different from internal cabin pressure) were accelerated changes in the aircraft center of gravity. Samples of their variations were calculated as the number of cycles in a specified period. Then the period was converted to equal values of 6000 flight cycles [8]. The final acceleration spectrum that the aircraft experience in the center of gravity is reported in Table C21 reference [8]. Considering the aircraft's fuselage as a cylindrical monocoque structure, numbers for the shear stresses in

longitudinal and circumferential directions were omitted and calculated as for a simple cylindrical pressurized vessel. Internal and external differential cabin pressure is related to aircraft altitude and is recorded in Table C20 in the reference [8]. The stress spectrum of the damaged location as the sum of two terms, the "stress spectrum in the center of gravity" and the "cabin pressure differential" in the longitudinal or circumferential direction of the fuselage could be calculated using Equation 1. This equation converts the general loading spectrum to a stress spectrum as obtained from Table C21 in reference [8].

$$\sigma = f(p) + f(g) = \sigma_p + (1 \pm \Delta g)\sigma_{1g} \quad (1)$$

Where:

σ : stress in longitudinal or circumferential direction at point of damage

σ_p : Stress in damage location because interval cabin pressure equals pr/t for longitudinal cracks and $pr/2t$ for circumferential cracks

σ_{1g} : Stress in damaged location as a result of aircraft inertia and aerodynamic loading

Δg : Load coefficient according to loading spectrum table

σ_{1g} : Stress defined in longitudinal direction based on maximum design stress, shown in the form of σ_{1gm} . It was assumed that maximum stress (σ_{1gm}) would occur at the upper crown plate of the wing panel while σ_{1g} would be zero at each end of the aircraft and zero distance [8]. The location of the selected component is shown in Fig. 13 and 4m from nose section. Finally the combination of different loadings and the stress spectrum in the damaged location would be based on the following diagram, shown in Fig. 14.

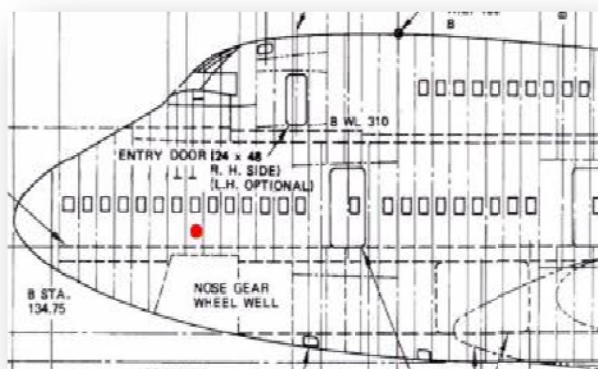


Figure 13. View of the location of damage for finding spectrum loading

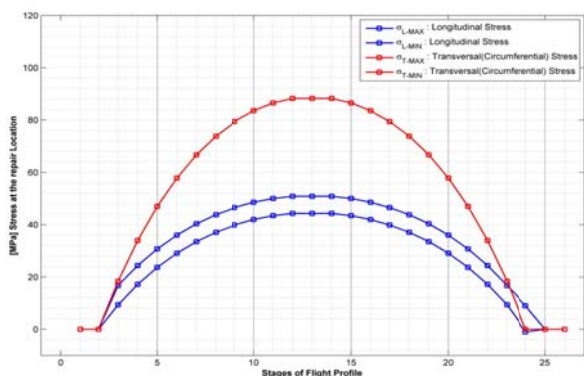


Figure 14. Sample of loading spectrum for location shown in Fig. 13

Finite Element Modeling and Analysis

One main point of fatigue analysis in fracture mechanics is to find the stress intensity factor at the crack tip. In order to find the stress intensity factor at that point, the finite element method was used. The subject was assumed to be two-dimensional.

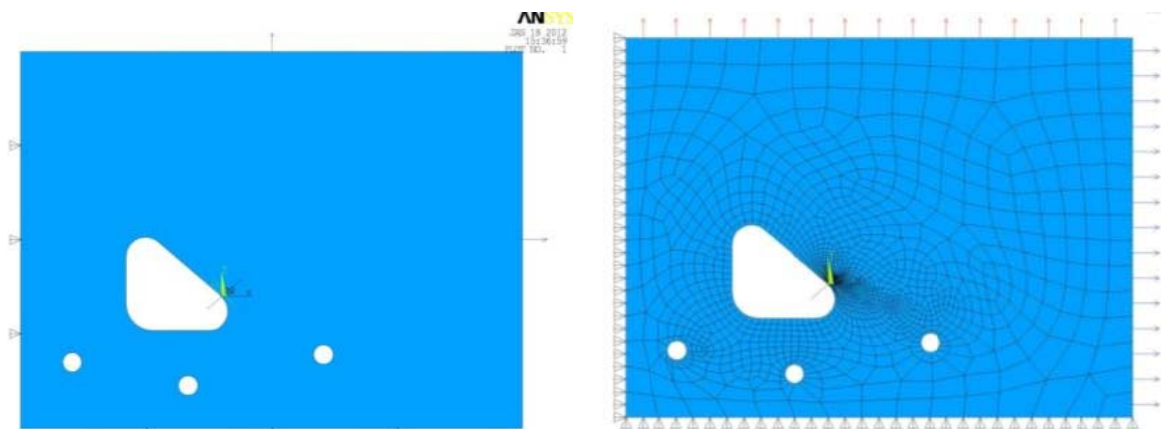


Figure 15. (a) Two dimensional models produced from initial 1 millimeter crack around designated hole (b) Mesh generation with second order elements accompanying boundary layer and loading condition

Critical and Initial Crack Lengths

The initial crack length was assumed 0.05 inch [8] and in fracture mechanics, if the crack tip stress intensity factor equals the fracture toughness of the material, then crack length will be critical. In this case, crack growth would be unstable and the crack is propagated with the speed of sound.

When the loading for crack growth is known and crack growth in the fatigue mechanism is well-defined, the unknown parameter is the length, and the stress intensity factor equals fracture toughness. In integrated structures, loading and stress are not the same everywhere. So, as a result, to find the critical crack length in the integrated structure, the crack length

Additionally, it was planned with similar holes, the same crack, the same boundary layer conditions and the loading was applied according to Fig. 15(a). The mentioned analyses were based on two-dimensional planetary stress, and the elements to be used were from the second order with 8 nodes. The calculation network is illustrated in Fig 15(b). The selected direction for crack propagation and loading in X and Y direction caused the crack to be propagated in composite mode and the stress intensity factor in the first and second mode (K_I and K_{II}). K_I and K_{II} were recalculated and for the evaluation of crack condition and application of Paris equation, the K_{eqv} (equivalent of K_I and K_{II}) was used. The K_{eqv} was calculated from equation (2) [11] and the results are shown in Fig 16. This diagram shows the stress intensity factor versus longitudinal stress in various crack sizes.

$$(K_{eqv})^2 = (K_I)^2 + \left(\frac{K_{II}}{0.75}\right)^2 \tag{2}$$

should be studied at critical points. Refer to ref [8] to see the critical points in the first zone fuselage are the end points of this area, meaning the threshold of wings. For critical length at arbitrary points of this area, the following procedure should be adopted:

- Calculate the stress field at the arbitrary point
- Specify the calculated stress field in the horizontal axis of Fig. 19
- Select the first curve under the K-IC of the material
- Read the corresponding number of the selected curve from guide diagram
- This number is critical crack length at the arbitrary point

For example, doing this procedure for 3 points on the critical section of the first zone fuselage means that end points/threshold of the wings and, as a result,

critical crack length for A, B, C points are 6 mm, 19 mm, and 10mm, respectively in Fig16.

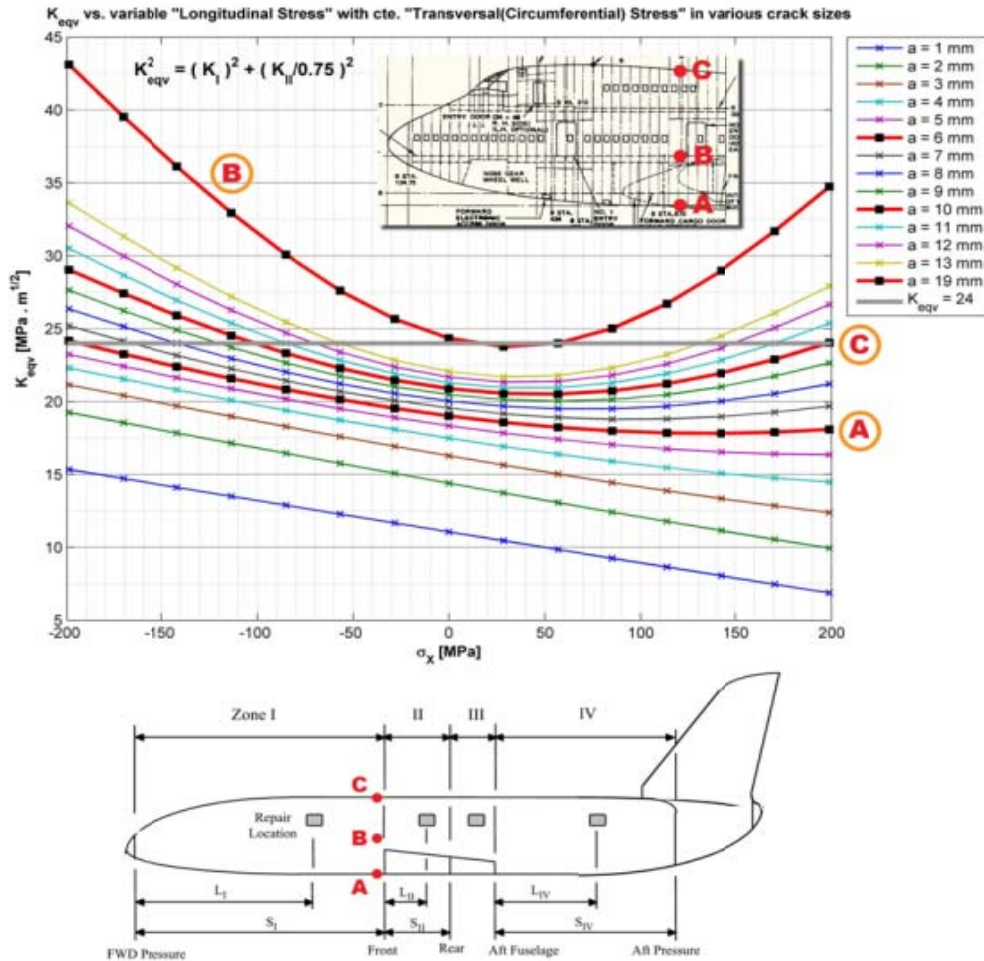


Figure 16. Critical crack length on the critical section of first zone fuselage

Location of Initial Crack

At this point, the initial crack length, crack direction, and critical crack length were determined. The investigation of this study showed that the stress level for crack propagation at point “O” in Fig. 17 is low, because point “O” is very close to the neutral axis (deck) and reduces the fluctuation range of the longitudinal bending Stress. Therefore, obviously the stress level of points A, B, C, D are more than point O for selected points. These are the highest potential for crack propagation, hence two features are considered:

- being far from neutral axis (deck)
- being near to end points/threshold of the wing in the faced zone fuselage

For this purpose, 4 points were selected. These points are shown in Fig.17, named A, B, C, D and marked by red, black, green, and blue, respectively. This coding was kept in all curves and diagrams.



Figure 17. Illustration of selected point for fatigue crack growth analysis

Fatigue Crack Growth Analysis

In order to calculate the component fatigue life limit from a fracture mechanics point of view, it was needed to consider the subject of fatigue crack growth. In the finite element analysis for crack growth modeling, we need the specific criteria (i.e. finite elements output data) which, in this field of study, are obtained from variable functions in structural analysis. In fact these variables are displacement. If a quantity such as stress, strain, or energy, which is related to these displacements, is considered in the final evaluation, the stress intensity factor which introduces fracture mechanics elasticity would help find the property that is in a linear situation with the field of stress at the final stage of the finite element analysis. With the aid of a model based on this property, we can achieve a certain indicator for fatigue crack growth. The item in accord with fatigue analysis from a fracture standpoint in the finite element method is, in fact, crack growth. In this case, using the model and growth criteria hand in the same result, and the fatigue crack rate (i.e. growth length in each loading cycle) would be drawn in the form of extremities of stress intensity factor variations at the point of the crack. Fatigue crack growth rate diagrams (i.e. crack length in each loading cycle) are presented for 3 types of aluminum based on the tensional stress variation of the coefficient extremity at the crack tip [9]. This logarithm diagram is divided into 3 zones which, for the intermediate zone (linear part) power equation, are known as Paris' law (Equation 3,4) [10, 11].

$$\frac{da}{dN} = f(k) \quad (3)$$

$$\frac{da}{dN} = c(\Delta k)^m \quad (4)$$

The material used for the aforementioned modeling was aluminum T6-7075 and the two constant values "c" and "m" were calculated while these two constant values for the proposed aluminum were selected as 3.6×10^{-11} and 4.1 [9]. Consequently, the part service life time was calculated with the integration in Equation 5 being per se derived from Equation (4) [10, 11].

$$N = \int_{a_i}^{a_f} \frac{1}{f(\Delta k)} da \quad (5)$$

By assuming the final crack a critical crack, its length will be located at the upper limit of the equation (5). In this equation, N would be the final service life of the component. The location and direction of the initial cracks in the structure will determine the amounts of the stress intensity factor during growth and consequently, by assuming a model $f(\Delta k)$ function, it would be possible to calculate the integral (4). The size and direction of initial crack is the same as the bigger crack, and the situation around the crack is the same as the component used for proposed modeling (bigger crack on right hand side of hole in Fig. 4). With respect

to the number of loading cycles being known, the calculation of crack growth was carried out. The calculation of the crack growth rate (Δa) in this number of cycles was considered and calculated using equation (6), and in this case integration of N would be made [10, 11].

$$a = \int_{N_1}^{N_2} f(\Delta k) dN \quad (6)$$

In other words, ten blocks of loading equaling 6000 cycles were applied to the model at each block. The sum of the block increment for each of them was calculated. Therefore loadings, except cabin differential pressure, were recalculated as a variation of acceleration at aircraft c.g for 6000 flight block, as reported in Table 21 in the reference [8]. Thus final acceleration spectrum which the aircraft would experience at c.g was calculated. This acceleration spectrum became fuselage longitudinal stress and after combining with longitudinal and lateral stress caused from internal cabin pressure, the stress spectrum for 1 period of 6000 flights was achieved. Therefore we would be able to do the same calculation for 10 blocks of 6000 flights.

If da/dN is a constant value, it is possible to calculate crack growth rate for 1 loading cycle (1 flight) and then multiply any number of cycles, which result in final length. In fact the practical method is to divide the number of spectrum cycles by 6000 flights, and the number of cycles for 8 different stages of each flight could be calculated. This helps the specified code to be capable of solving the finite element model for 6000 flights and causes the exact number of flights required for cracking to reach the required specified length.

The worst and most unrealistic method is to apply 60000 flights simultaneously in order to make the crack reach critical distance, because it is not possible to distinguish at what number of flights critical value is recorded. The nominal method for solving this problem is to divide 60000 flights into 10 different parts and the final crack length in each stage of the initial crack would be the default value for the next stage. Each of the ten parts consists of 8 loading blocks. In each block there exist 6000 flight cycles. For example, at the first block there are 6000 aircraft surface movements before commencing the flight, and in the second block there are 6000 takeoffs, and the situation is the same for climb, cruise, landing, and surface movement after landing and flight. Consider, if the crack for the fifth period of loading reaches critical value, that event would occur between 24000 and 30000 flights. In order to find the precise number of failure situations, it is possible to increase the number of loading periods, for example to increase 10 periods of 6000 block 60 of 1000 block will help calculate the results for less than 1000 flights.

In Fig.18, the stress intensity factor at maximum and minimum loading for 60000 flights is as illustrated for the 4 points of A, B, C, and D at the first zone of the fuselage. Also in the landing phase an excessive load would be applied to the fuselage, but as interior cabin pressure approaches zero, there is no sign of increase in stress values. For k_{eqv} as we see in Fig.19, from maximum and minimum values it is possible to find the range of variation in k_{eqv} values.

In Fig.20 we can see Δk_{eqv} for 60000 flight cycles of 4 specified points at the first zone of fuselage. The limit for cruise flight and landing of aircraft can also be seen in the diagram. One period of calculation consisting of 6000 flights of 54000 to 60000 flight cycles for 4 points at the first zone of the fuselage is shown in Fig.21. The main point which should be noticed in comparing Figs.19 and 21 is the significant situation for Δk_{eqv} at the landing phase and the k_{eqv} during cruising conditions. As we can see, the fuselage experiences the most deviation of stress intensity factor during landing phase of the flight; but that does not mean that most crack growth occur during this phase of the aircraft. By referring to reference [8] table 21, we can see that, for 6000 flights the aircraft will experience 6.8 million cycles, but for the aircraft landing phase, only 6000 cycles is applied during 6000 flights. That is to mean that in each flight more than 1 million cycles of variation in the Δk_{eqv} domain is applied to the fuselage while it cruises, but Δk_{eqv} for the landing phase occurs only once. For this reason, in order to have a share of each stage of flight represented in crack growth it is better to apply the number of cycles in the calculations.

Fig.22 shows the crack growth rate with an initial length of 1 millimeter for assigned points. As we see, crack growth during the aircraft landing phase (third point from right) is approaching zero. In Fig.23 (a, b), crack growth variation based on each phase of flight is shown. It is obvious that a crack with an initial length of 1 millimeter at point A and B does not have considerable variation (the red and black curves). In point C the range of variation is small and rises incrementally with increases in crack length. Even at point D crack length shows no considerable changes, and it is possible to see ascending and descending trends for Δa . If the calculation of the flights is continued for more than 60000, once again the trend of changes increases. This significant change for Δa is a result of stress effect respecting the location of the crack. The stress situation at the tip of the crack changes continually, however. In Fig.24, Δa variation of values can be seen. Also in Fig. 25 these parameters are illustrated in integrated form, including the 1 millimeter initial length of the crack. As we can see, cracks with an initial length of 1 millimeter will increase to 3 millimeters as a result of 60000 flight cycles. By limiting flights to 6000, the crack growth value for 6000 cruise flights can be seen. In order to distinguish the trends of change for crack length as shown in Fig.24, the points for the end of each of the 6000 flights is presented.

In Fig. 25, the fatigue crack growth curves are compared with linear conditions, and it is obvious that as a result of less crack growth, the trend of these changes approaches linear conditions. In case of a continued increase in cyclic loading, the growth trend would leave the linear situation, and its shape would depend on the length of the crack. In addition, we see that at no point would the crack reach the critical length.

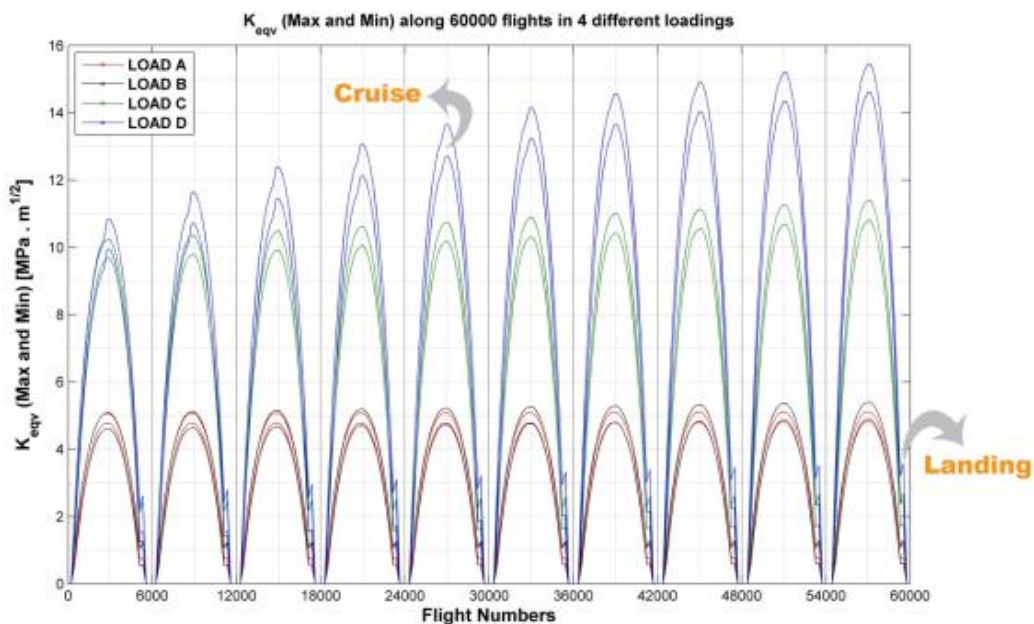


Figure 18. equivalent stress intensity coefficient at maximum and minimum loading of 60000 flights for 4 points at the first zone of fuselage

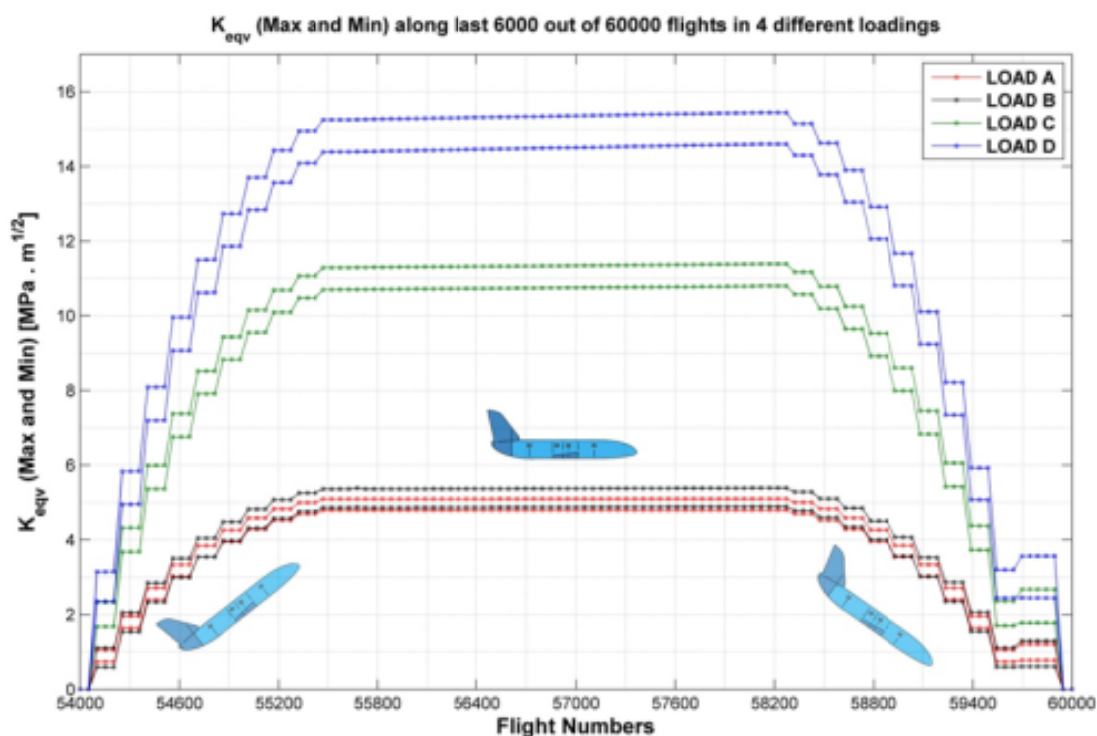


Figure 19. Equivalent stress intensity coefficient at minimum and maximum loading in 1 period of calculation, on 6000 flights from 54000 to 60000 on 4 points at the first zone of fuselage

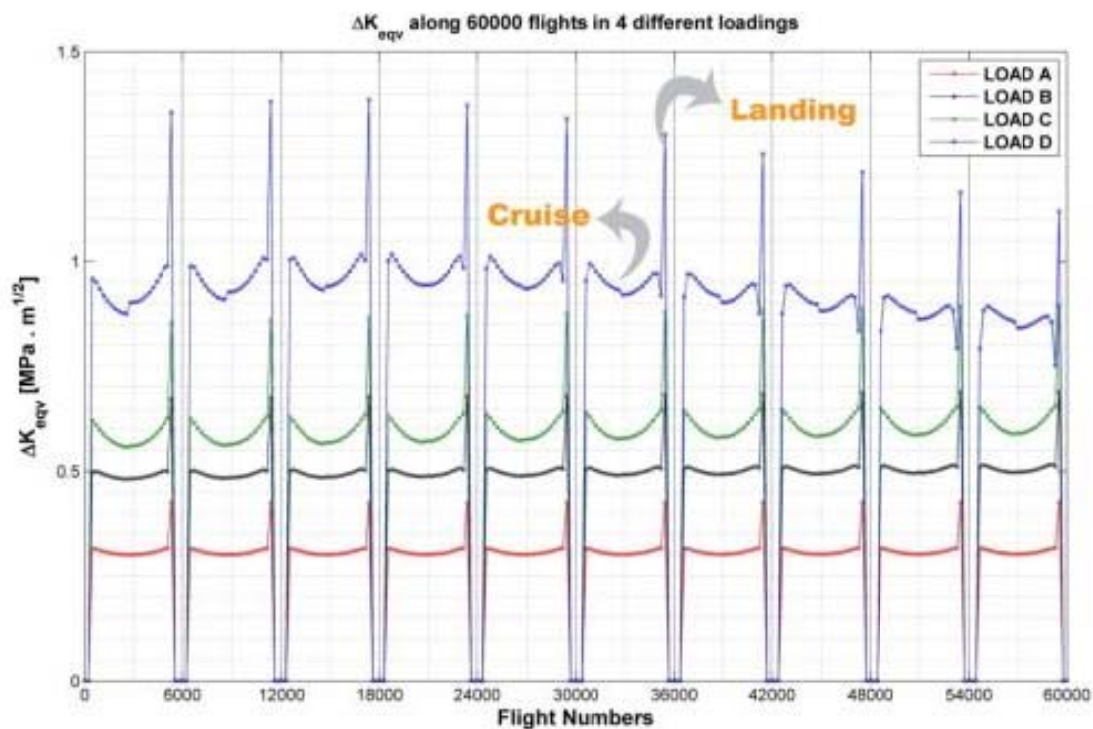


Figure 20. Equivalent domain of stress intensity coefficient changes for 60000 flights on 4 points at the first zone of fuselage

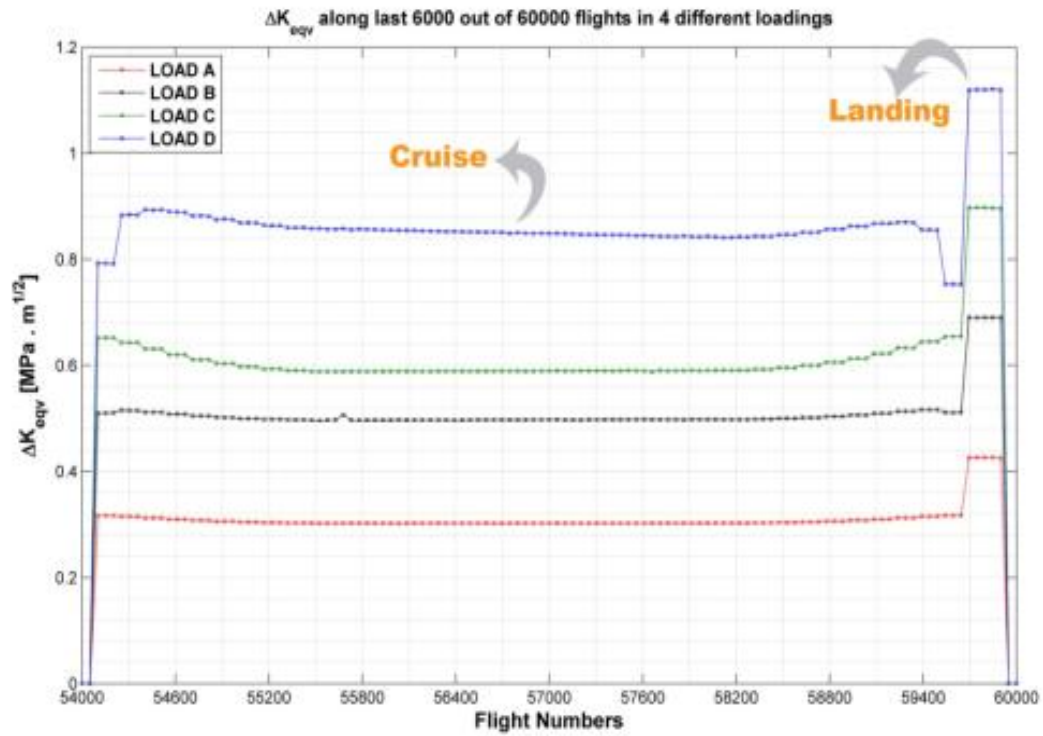


Figure 21. The equivalent domain for stress intensity coefficient changes during 1 period of calculation, on 6000 flights from 54000 to 60000 flights on 4 points at the first zone of fuselage

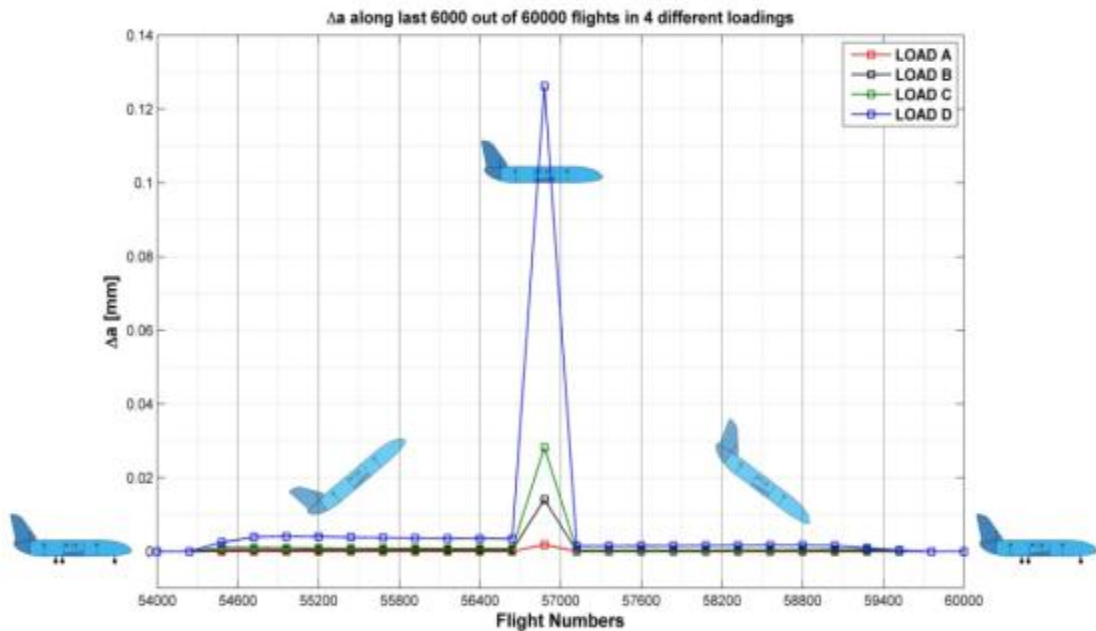


Figure 22. Crack growth rate with initial length of 1 millimeter during 1 period of calculation, on 6000 flights from 54000 to 60000 flights on 4 points at the first zone of fuselage

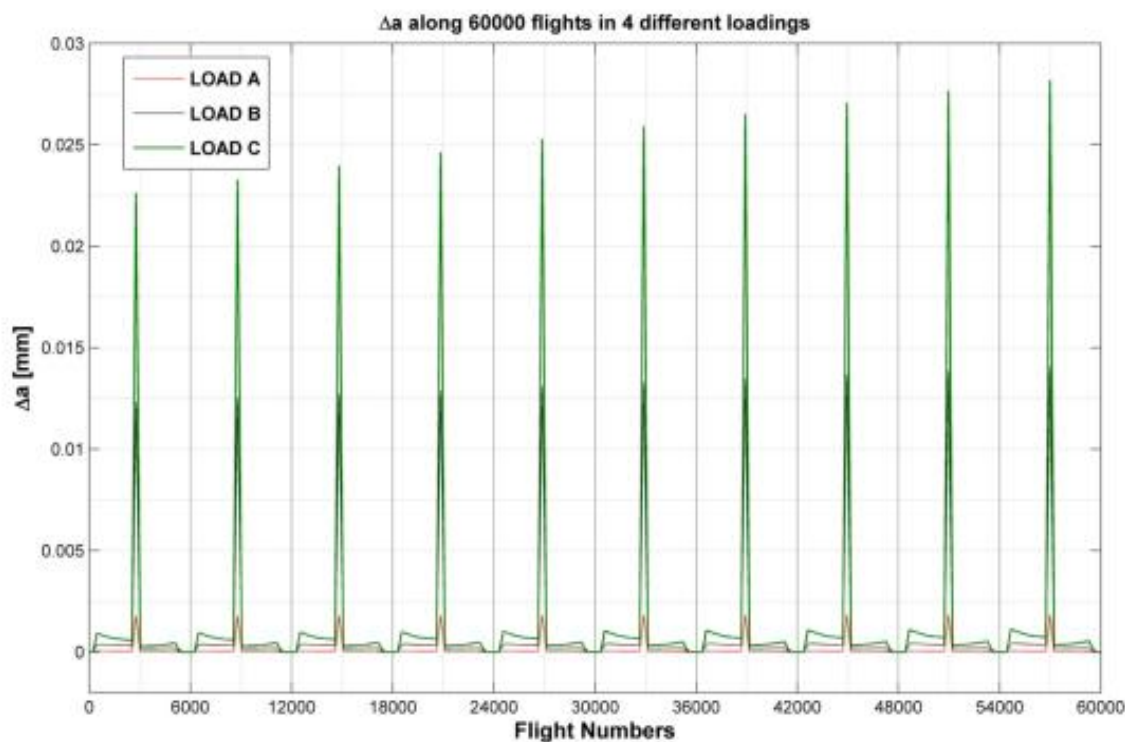
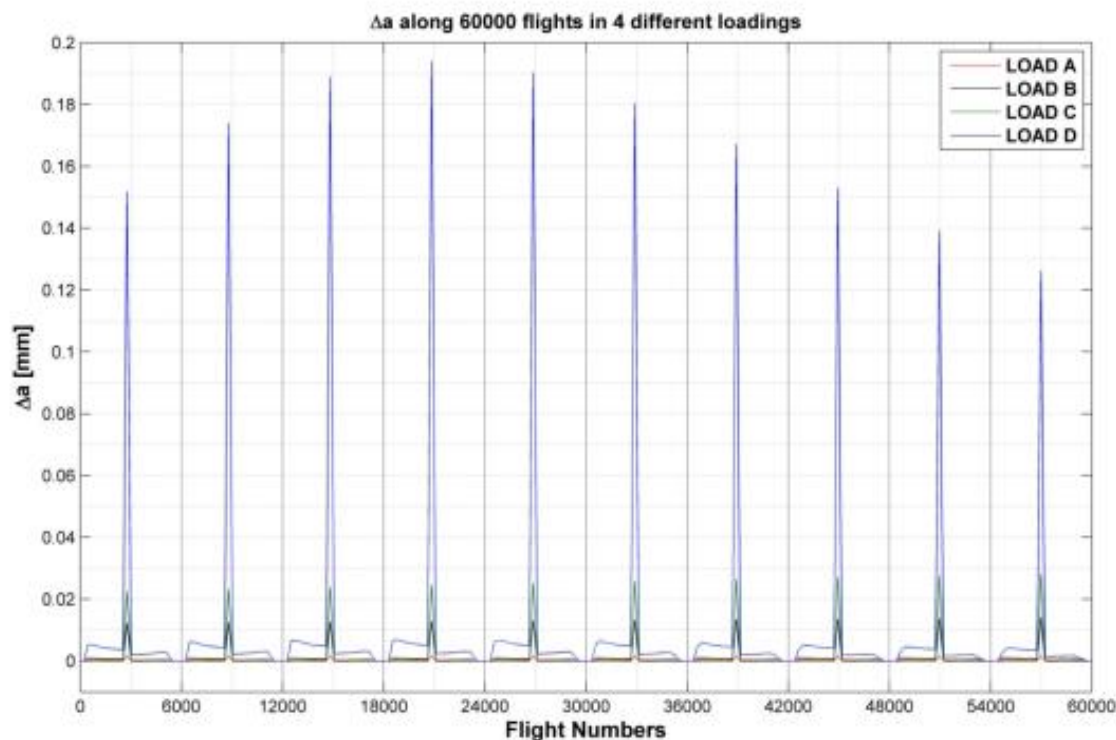


Figure 23. (a, b). Crack growth rate for initial crack of 1 millimeter of sample during 60000 flights on 4 points at first zone of fuselage

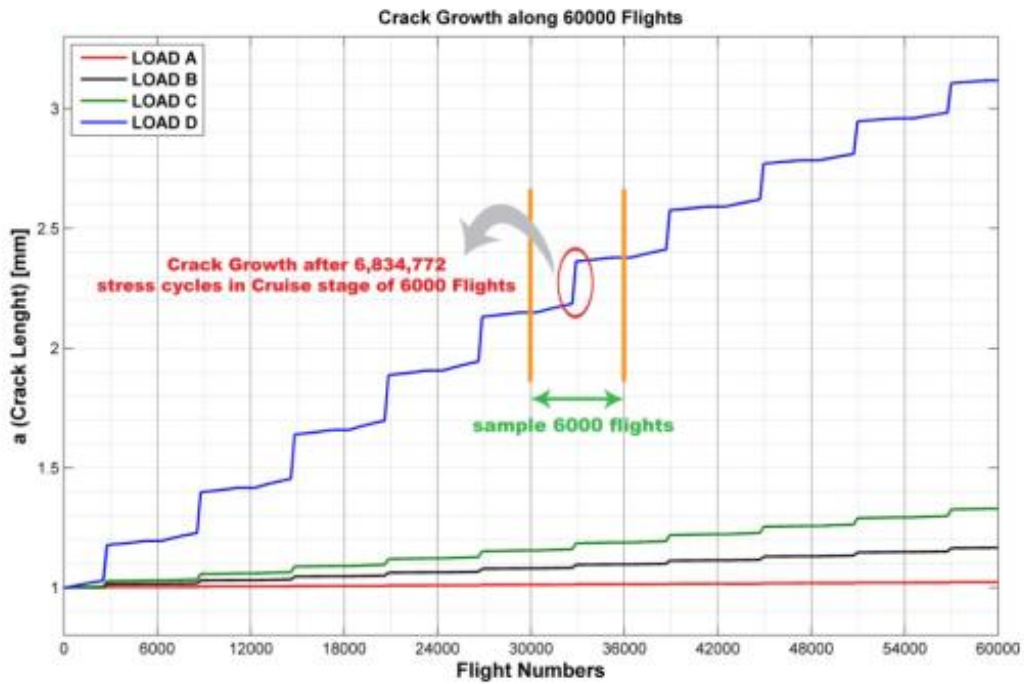


Figure 24. Crack length value of first 1 millimeters of sample as a result of 60000 flights on 4 points at the first zone of the fuselage

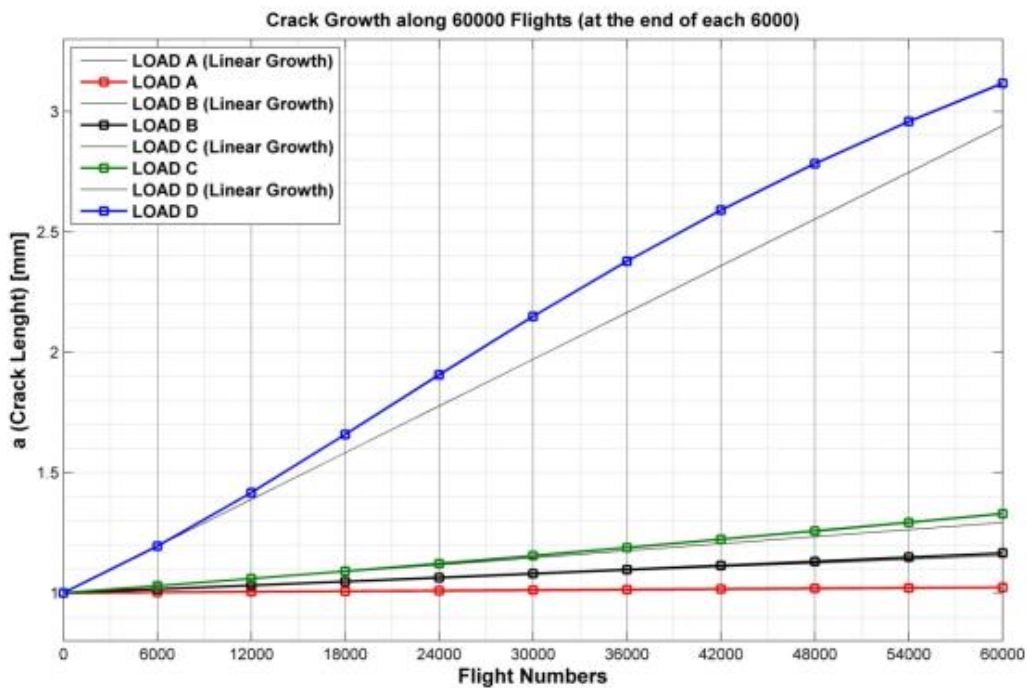


Figure 25. Crack length value of first 1 millimeters of sample as a result of 60000 flights on 4 points at the first zone of the fuselage

Conclusion

The best ways to promote an aircraft structural design and maintenance program could be using the MSG-3

process (on structure). This process is based on LDP and covers the accidental, environmental and fatigue damages for SSI and other structural items. In this article we investigated the MSG-3 process for SSI

components. For this purpose fractography and the crack growth analyses by FEM were used. In the selected component and for smaller crack the result of fractography for the surface fracture indicated that the lead crack initiation growth rate and also for bigger crack under life limit cyclic loading in none of the selected points the crack would reach the critical length; hence, specified periodic inspection would be done. As mentioned before, the MSG-3 process covers all damage types. In future plan the first step for promoting the maintenance program in structure field is that all cracks in SSI components are going to be placed under investigation in selected aircraft to cover the fatigue damage and then the plan on the other components and damages type will be developed.

REFERENCES

1. Shannon, P. Ackert, "Basics of Aircraft Maintenance Programs for Financiers," Date of Issue: October 1, 2010 www.aircraftmonitor.com
2. ATA (Air Transport Association) "MSG-3 Operator/Manufacturer Scheduled Maintenance Development" revised 2003.
3. Mosinyi, Bakuckas, Awerbuch, Lau, Tan "Crack Growth Assessment of High-Usage in-Service Aircraft Fuselage Structure," Drexel University / FAA / Delta Airline -Aging Aircraft Conference FAA/DOD 2005.
4. John G. Bakuckas, Jr - Aubrey Carter "Destructive Evaluation and Extended Fatigue Testing of Retired Aircraft Fuselage Structure," Proceedings of the 6th Joint FAA/DoD/NASA Conference on Aging Aircraft, September 2002, San Francisco, CA
5. John G. Bakuckas, Jr - Aubrey Carter "Destructive Evaluation and Extended Fatigue Testing of Retired," Aircraft Fuselage Structure: Project Update Proceedings of the 7th Joint DoD/FAA/NASA Conference on Aging Aircraft, New Orleans, Louisiana, September 2003,
6. BOEING COMPANY "SRM (Structure Repair Manual)- D6-13592 B747" 2010
7. McEvily A.J. and Matsunaga, H., "On Fatigue Striations," Scientia Iranica Vol. 17, No. 1. Sharif University of Technology, February 2010.
8. FAA and USAF "RAPID (Repair Assessment Procedure and Integrated Design)" Version 2.1. May 1998.
9. ALCOA Co "Alloy 7075 Technical Sheet, www.millproducts-alcoa.com"
10. A. G, Grandt, *Fundamental of Structural Integrity*, Wiley and Sons 2003.
11. Broek, David, "Fracture Mechanics," The Practical Use, 1988.